

Ultrafast Carrier Redistribution in Single InAs Quantum Dots Mediated by Wetting-Layer Dynamics

Mattias Johnsson,^{1,2} David Rivas Góngora,³ Juan P. Martínez-Pastor,⁴ Thomas Volz,^{1,2} Luca Seravalli,⁵ Giovanna Trevisi,⁵ Paola Frigeri,⁵ and Guillermo Muñoz-Matutano^{1,2,*}

¹Department of Physics and Astronomy, Macquarie University, New South Wales 2109, Australia

²ARC Centre of Excellence for Quantum Engineering, Macquarie University, New South Wales 2109, Australia

³Institute of Physics, Bijenicka cesta 46, Zagreb HR-10000, Croatia

⁴UMDO (Unidad Asociada al CSIC-IMM), Instituto de Ciencia de Materiales, Universidad de Valencia, P.O. Box 22085, Valencia 4607, Spain

⁵CNR-IMEM Institute, Parco delle Scienze 37a, Parma I-43100, Italy



(Received 15 January 2019; revised manuscript received 18 March 2019; published 15 May 2019)

Optical studies of single self-assembled semiconductor quantum dots (QDs) have been a topic of intensive investigation over the past two decades. Due to their solid-state nature, their electronic and optical emission properties are affected by the particular crystal structure as well as many-body-carrier interactions and dynamics. In this work, we use a master equation for microstates (MEM) model to study the carrier capture and escape from single QDs under optical nonresonant excitation and under the influence of a two-dimensional (2D) carrier reservoir (the wetting layer). This model reproduces carrier dynamics from power-dependent and time-resolved microphotoluminescence experiments. Due to the random nature of the carrier capture and escape processes, when a single QD is pumped with enough excitation power, the carrier redistribution across the available QD microstates produces an effective double-peaked excitonic decay. This double peak is characterized by a first ultrafast (subnanosecond) and a second conventional (approximately nanosecond) decay. The effective transient photoluminescence shape of the population dynamics is governed by the wetting-layer radiative decay and the exciton capture time.

DOI: 10.1103/PhysRevApplied.11.054043

I. INTRODUCTION

Emerging quantum technologies depend on the design of realistic proposals to implement and control quantum correlations [1]. The development of these technologies depends to a large extent on the control and manipulation of individual quantum systems. Single self-assembled semiconductor quantum dots (QDs) have been extensively proposed as artificial atoms for quantum-optics and photonics applications, and are one of the most successful solid-state systems for developing single-photon sources [2–6]. However, semiconductor QD-carrier dynamics are complex processes due to the interaction between the QD and its local and crystal environment, which can lead to undesired effects, decreasing the quality and efficiency of the single-photon sources.

In epitaxial QDs, the complexity is increased by the self-assembled growth mechanism. InAs QDs are grown via strain-relaxation processes in lattice-mismatched

semiconductor heterostructures. After the active InAs layers reach a critical thickness, zero-dimensional (0D) island strain-driven growth starts. This QD growth process builds an intermediate two-dimensional (2D) strained InAs thin layer, known as a wetting layer (WL), between the InAs QDs and the GaAs substrate. The interaction between the QD states and the WL state has been a research topic since these nanostructures were first proposed. Among other effects, it has been shown that WL interaction affects the dephasing time in quantum dots [7], builds a carrier-redistribution channel as a function of the sample temperature [8], enables the possible coupling between adjacent QDs [9], and shifts the energy of QD states [10] and their intersubband *P*-to-*S* transitions [11]. Furthermore, the WL state offers an important carrier thermal escape, and transport channel [12–15] and affects the carrier relaxation and capture to QDs by virtue of the WL carrier diffusion processes [16,17]. In essence, interaction between the 2D-WL and 0D-QD states offers a complex scenario that must be taken into account to describe specific carrier dynamics in these kinds of artificial atom platforms. The correct modeling and description of these dynamics will be important

*guillermo.munozmatutano@mq.edu.au

for the actual development of QD laser operation [18–20], all-optical QD-based processors [21], and the on-chip integration capabilities of single-photon emitters [22–26], as well as many other applications.

Time-resolved techniques have been extensively employed as an optical characterization tool to study semiconductor carrier dynamics [27,28]. QD optical transients return information about multiexcitonic decay recombination [29–33], exciton formation times [34–36], exciton dephasing processes [37–39], spin- and dark-state-relaxation processes [40], and QD size, structural, and composition properties [41–43], among other examples. When analysing time-resolved photoluminescence (TRPL) emission as a function of the excitation power, previous studies have shown a double-peak structure in the various QD excitonic-complex decay traces [29,30,41,44–49]. The double-peak structure is composed of a first fast decay (< ns) followed by a second and slower decay (approximately nanosecond duration) and has been associated with excited and dark-state refilling processes [44,50], multiexciton recombination ladders [29,30,47], and WL-to-QD ground-state interactions [41,45]. This double-peaked excitonic decay can be one of the factors in reducing the single-photon purity quality of the emission when the nonresonant pumping is pushed to the desired brighter rates [51,52].

In this work, we measure spectral, time-resolved, and photon correlation features from the optical emission of single InAs QDs when pumping with nonresonant excitation as a function of the power. We find double-peaked transients when exciting close to the saturation threshold, both in the neutral exciton and in the single positively charged exciton (positive trion). We use a master equation for microstates (MEM) model to study the carrier capture and escape from single QDs under nonresonant excitation and including the interaction with the WL state, simulating both steady state optical time transients and the second-order correlation function [$g^{(2)}(\tau)$]. Our model reproduces the PL-integrated-intensity power evolution and the double-peak structure in the temporal PL transients, where the exciton, electron, and hole capture and escape times have been considered as constants. Fitting the model to the experimental data allows us to extract capture and escape times, as well as the ratio of excitons to electrons or holes that are created as a function of the excitation power. Our results demonstrate that a simple model describing the carrier feeding from the WL reservoir to the different microstate configurations using an *s*-level QD approximation reproduces the double-peaked decay and explains the particular dynamics without the presence of any excited, dark, or higher-order multiexcitonic states. The rich number of carrier configurations present in the simplest QD-state architecture modulated by the WL dynamics could lead to substantial microstate-refilling processes.

II. SETUP AND SAMPLES

The QD sample is grown by molecular beam epitaxy (MBE) on a semi-insulating (SI) GaAs substrate. Atop a 100-nm-thick GaAs buffer, InAs is deposited at a low growth rate (0.009 ML/s) at 535 °C, with an equivalent coverage of 2.5 MLs. The InAs growth rate is calibrated by recording the time for the QD formation using reflection high-energy electron diffraction (RHEED), taken at 460 °C. XRD characterization demonstrates that the WL is composed of an $\text{In}_{1-x}\text{Ga}_x\text{As}$ alloy rather than by pure InAs, with x taking values around 0.80 [53]. The growth ends with another 100-nm-thick GaAs cap, grown by atomic-layer MBE at 360 °C [54]. For the whole MBE growth, tetramer arsenic species is used. During the InAs deposition, the substrate is not azimuthally rotated, thus obtaining a continuous variation of the InAs coverage throughout the sample surface [55]. These conditions result in a density of InAs QDs of about 16 QDs per square micrometer, as estimated by atomic-force microscopy (AFM) carried out on uncapped samples grown under the same conditions [56]. The AFM images show a bimodal distribution of QDs: large QDs have heights of 14 nm and diameters of 54 nm, while smaller QDs have heights of 9 nm and diameters of 36 nm. Both types of QD have a symmetrical half-domed shape. Information about AFM and ensemble photoluminescence characterization can be found elsewhere [15].

We use a cw laser diode operated at 790 nm as the excitation source in the microphotoluminescence (μ -PL) spectral analysis and a pulsed laser diode emitting at 790 nm for time-resolved μ -PL (μ -TRPL) analysis. The laser beam is coupled to an optical fiber and carried to the excitation arm of a diffraction-limited confocal microscope (spot diameter approximately 1.2 μm), working at liquid-helium temperature (4 K). The μ -PL signal is coupled to the collection arm of the confocal microscope and attached to a single-mode optical fiber. An Andor Technology CCD is attached at the front output of a double 0.3-m Princeton Instruments monochromator in order to record the μ -PL spectra, whereas a silicon Perkin Elmer avalanche photodiode (APD) is attached to the intermediate output of this monochromator (with 70 μeV spectral resolution). The μ -TRPL is measured by means of filtering the PL by the monochromator and connecting the laser trigger and the TTL output of the APD to the start and stop channels of a T9000 time-correlated single-photon counting (TCSPC) card from Edinburgh Instruments (producing a final experimental time response of approximately 400 ps). Photon correlation is measured dividing the optical signal using a 50:50 fiber beam splitter. The signal in each arm is filtered by two independent monochromators and finally detected by APDs. The APD electrical output signal from each APD is connected to the start and stop channels of the TCSPC.

III. THE MODEL

In order to obtain quantitative information about the QD-carrier dynamics, we model μ -PL and μ -TRPL spectra by using a MEM model, which is based on random QD-carrier capture and recombination. In this kind of model, the probability of finding the QD in a particular charge configuration, called the microstate, is computed. A particular microstate describes the QD at any time with a well-defined number of electrons (i) and holes (j). For simplicity, we reduce the QD levels under consideration to S states (for electrons and holes), which means that we do not study transitions that involve more than two electrons and/or two holes.

Figure 1(a) represents the QD state in terms of microstates and shows population flows between them. We define $\eta_{ij}(t)$ (where $i,j = 0, 1, 2$) as the probability of the system being in a particular microstate at time t , with i corresponding to the number of electrons and j corresponding to the number of holes. This means that the excitonic complexes are the microstates with both i

and $j > 0$ ($\eta_{11} = X^0$, $\eta_{21} = X^{-1}$, $\eta_{22} = X^{+1}$, and $\eta_{22} = XX^0$). The total summation of the microstate probabilities must be normalized to 1. As a consequence, the losses in population of one microstate (by carrier capture or/and escape) result in an increase of the population of another microstate. The arrows in Fig. 1(a) refer to all possible radiative and nonradiative transitions from one microstate to another. τ_{ce} and τ_{ch} are capture times for electrons (downward vertical arrows) and holes (rightward horizontal arrows) respectively, τ_{ee} and τ_{eh} are electron (upward vertical arrows) and hole (leftward horizontal arrows) escape times, τ_x is the exciton capture time, and τ is the radiative lifetime for the different exciton species (represented with diagonal arrows). The QD is connected to a carrier reservoir (WL) and from this reservoir excitons and $e-h$ pairs are pumped into the QD [Fig. 1(b)]. For this reason, three different WL-level structures are considered (W_e , W_h , and W_X). Here, W_X does not refer to the excitonic level of the WL but to the exciton reservoir in the WL. In our model, we are just including three different carrier-injection paths from the WL, associated

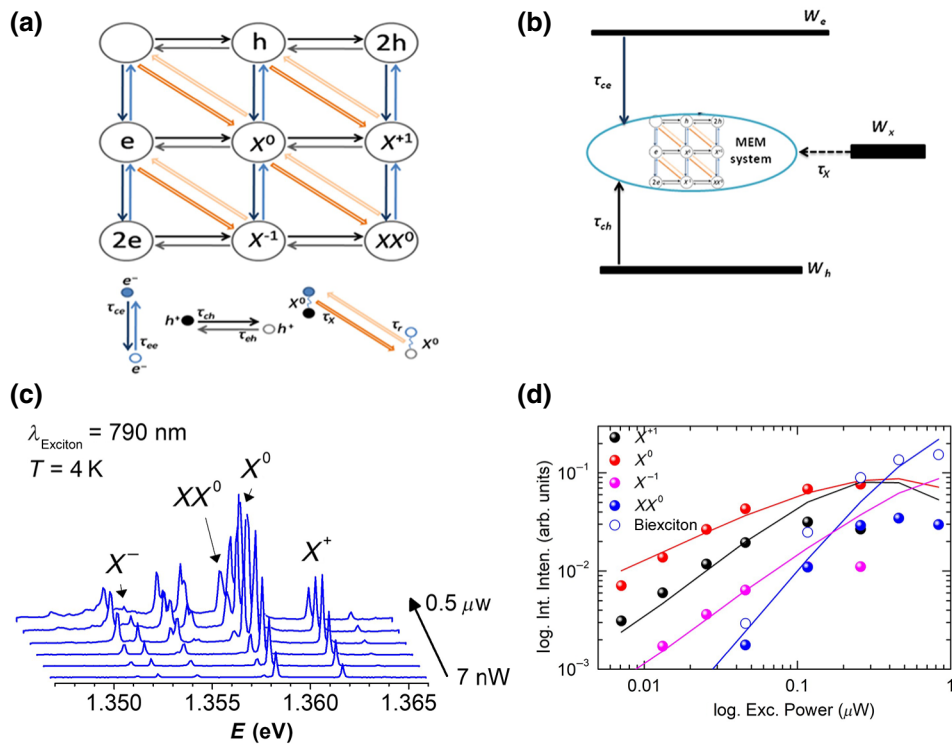


FIG. 1. (a) A microstate scheme of all the different charge configurations of a single QD represented by our MEM model. Vertical arrows correspond to single electron capture (downward) and escape (upward). Horizontal arrows correspond to single hole capture (right) and escape (left). Diagonal arrows correspond to the capture of an exciton (downward) and to radiative recombination (upward). (b) The interaction between the QD and the WL carrier reservoir for excitons, electrons, and holes. (c) A single QD microphotoluminescence spectrum as a function of the excitation power, with cw nonresonant pumping configuration at 4 K. The mean excitonic transitions are labeled as neutral exciton (X^0), neutral biexciton (XX^0), negative trion (X^{-1}), and positive trion (X^{+1}). (d) The experimental integrated intensity as a function of the cw excitation power (colored dots) and the model simulation (continuous lines) for the main excitonic transitions in a double-logarithmic plot. The calculated number of injected carriers at various cw powers is 1.2×10^8 carriers/s (0.01 μW), which is estimated considering the GaAs capping-layer thickness, the spot size, and the sample QD density. This value is very close to the estimate based on the carrier diffusion length.

with different capture times: (1) single-exciton injection, (2) single-electron injection, and (3) single-hole injection. Hence, W_X feeds the QD microstate network with one electron and one hole synchronously. However, W_e/W_h will inject one electron and/or hole with an independent time constant (nonsynchronous electron and hole capture).

Our model also includes electron and hole escape times (τ_{ee} , τ_{eh}) to describe carrier escape out of the QD through either deep levels (DL) or interface defects [57–59], the characteristic times of which have a strong influence on the total regeneration time of the excitonic complexes. It has previously been shown that *EL2* defects in GaAs and (In, Ga)As extended defects close to the QDs appear at $E_c - 0.74$ eV and $E_c - 0.61$ eV [60,61]. Spontaneous carrier escape from QDs to these levels can be described by phonon-assisted tunneling. As a consequence, the associated escape times should be long compared to the rest of the time constants in the model. However, we do not include any carrier escape from QD microstates to the WL reservoir, as thermal escape at 4 K is suppressed.

This model is described by a set of coupled differential equations in terms of the microstate probabilities and the reservoir levels, given by the following:

$$\begin{aligned} \frac{d\eta_{ij}}{dt} &= R_{ij}^X W_X + R_{ij}^e W_e + R_{ij}^h W_h + R_{ij}^{ee} + R_{ij}^{eh} \\ &\quad + R_{ij}^{\text{ID}} + R_{ij}^r, \end{aligned} \quad (1)$$

$$\frac{dW_X}{dt} = - \sum_{ij} E_{ij} R_{ij}^X W_X - \frac{W_X}{\tau_W} + G_a, \quad (2)$$

$$\frac{dW_e}{dt} = - \sum_{ij} i R_{ij}^e W_e - \frac{W_e}{\tau_W} + G_b, \quad (3)$$

$$\frac{dW_h}{dt} = - \sum_{ij} j R_{ij}^h W_h - \frac{W_h}{\tau_W} + G_b. \quad (4)$$

The R_{ij} are defined in terms of the capture, escape, and radiative decay times. A full description of the R_{ij} terms and the model as a whole can be found in Ref. [62,63]. The G_a and G_b terms correspond to the pumping of the reservoir by the optical excitation pulse, creating excitons or electron and hole noncorrelated pairs. The ratio between these pumping strengths will vary with the applied wavelength. In our model, these are linear in power, with a small constant offset arising from the unbalanced initial single carrier concentration due to the presence of ionized background impurities [56,64,65].

This set of equations is solved numerically using the open-source software package Xmds2 [66]. In the case of cw excitation, the simulations are run until steady state is reached, and in the case of pulsed excitation, 10 pulses are run in advance of the actual pulse of interest, as

this is the time required for the interpulse dynamics to become consistent with the recombination dynamics under a periodic pulsed excitation.

The experimental inputs to the model are the measured radiative time decays of each excitonic transition and the integrated intensity as a function of the cw excitation power, while the capture and escape times are considered as free-fitting parameters, although their general magnitudes are chosen to be consistent with previous work [62,63]. The relative strength of G_a and G_b is also considered to be a fitting parameter.

We stress that, once fitted, the same values are used for all simulations, regardless of whether the excitation is pulsed or cw. The capture times and escape times are taken as constant over the entire power-excitation range. This is an important feature of our model, as the carrier dynamics have previously been explained by power-excitation-dependent capture times [65], by nonsynchronous electron and hole capture processes [67], or by excitation-wavelength-dependent conditions [68]. More detailed information on the model can be found elsewhere [62,63,69].

The time constants obtained from fitting the model to the experimental data are shown in Table I. The form of the pumping terms is best fitted by the following:

$$G_a = 6\alpha P + 0.005, \quad (5)$$

$$G_b = \alpha P + 0.015, \quad (6)$$

where $P(t)$ is the time-dependent excitation-laser power in microwatts and α is a constant scaling factor to account for the efficiency of the conversion of photons into excitons or electron and hole pairs with 790-nm laser excitation. α also takes into account our inability to determine exactly how much power is being delivered to the quantum dots in the sample. While G_a and G_b are linear in power, the ratio G_a/G_b is power dependent (predominantly at low powers) due to the constant offset terms, which agrees with our previous results [63]. The changing of individual time constants affects multiple overlapping features of the dynamics, meaning that their effects are not independent and cannot be individually disentangled. In the TRPL data, however, the effects of the exciton capture time τ_X and the WL time τ_W on the X^0 , X^+ , and X^- populations are particularly clear, as will be explained below.

TABLE I. Time constants derived from the model by fitting experimental data. The same time constants are used for both the pulsed and the cw experiments.

τ_X	τ_{ce}	τ_{ch}	τ_{ee}	τ_{eh}	τ_W
80 ps	20 ps	70 ps	8.5 ns	27.0 ns	250 ps

IV. EXPERIMENTAL RESULTS

Due to the 0D density of states and the Coulomb interaction between carriers, typical single-QD spectra present a discrete set of sharp peaks, which arise from the exciton or multiexciton recombination. The basic excitonic recombinations in the QD are the neutral exciton (X^0), the biexciton (two electrons and two holes, XX^0), and the trion (a single positively or negatively charged exciton: X^{+1} / X^{-1}). The QDs present in our sample have typical μ -PL spectra composed of these excitonic and multiexcitonic transitions, as shown in Fig. 1(c). To label these excitonic transitions, we use all of the experimental data sets, consisting of power-excitation- and wavelength-dependent μ -PL spectra (not shown here) [56,63] and μ -TRPL transients. However, as shown in Fig. 1(c), the real dynamics of the QD under study presents a higher variety of carrier configurations, leading to a large number of optical transitions, which come from higher-order multiexcitons or hot-state recombinations [70–72]. In order to simulate this rich optical structure, the model should consider electron and hole p -states in the QD. An improvement of our model to include p -states in the QD would require a minimum of seven extra states: in addition, the inclusion of the electron and hole spin degrees of freedom is highly desirable, leading to a degree of complexity that goes beyond the scope of the present work. We also note that the experimental intensity of these extra transitions is too low to allow for complete experimental identification and lifetime characterization.

For these reasons, we restrict ourselves to a model that does not include QD p -states. As shown below, however, this still gives excellent agreement between our model and the experimental results at low and moderate powers, and allows us to obtain important information about the physics of the system and explain the behavior of the QD-carrier dynamics.

First, we measure and analyse the QD steady-state PL dependence as a function of the excitation power. Figure 1(d) shows the integrated experimental μ -PL (with colored filled dots) as a function of the cw laser-excitation power for the X^0 , X^{+1} , X^{-1} , and XX^0 transitions. The predictions of our theoretical microstate model are shown as a function of the same cw power range (solid lines).

The agreement between model and experiment is remarkably good for low and intermediate excitation powers. However, the model fails to reproduce the QD-carrier filling accurately at higher powers where saturation is reached, as shown by the discrepancy in both the X^+/X^- and XX^0 trends. These three QD transitions are at the limits of our simple model [Fig. 1(a)] and hence when the QD is pumped under high power, our model fails to reproduce the real carrier capture and/or escape to a multiexcitonic or a hot-QD microstate configuration, as these states lie off the edges of our model. To demonstrate this, Fig. 1(d)

plots the experimental integrated μ -PL intensity from all biexcitonic transitions in the QD spectrum (open circles), which are identified by the superlinear trend of the PL integrated intensity as a function of the excitation power. In this case, the agreement between experiment and model is quite good even at high pumping rates. Although the model only qualitatively reproduces these results, it provides an explanation for the physical origin of the deviation from the experimental trend, i.e., the existence of multiple biexcitonic transitions. At higher powers, all of the population in the model simulations will end up in the XX^0 state, as this is the highest-order complex available and should effectively be compared to the summed population of all the possible biexcitonic complexes seen experimentally.

As a second experiment, we measure the transient QD-state dynamics by means of μ -TRPL as a function of the pulsed laser power. Figures 2(a) and 2(b) show the X^0 and X^{+1} μ -TRPL excitation power evolution (open circles) and the simulation of the time dependence of the occupation probability (red continuous lines). Both states show similar dynamical evolution. We see the conventional single exponential decay of approximately 1 ns when exciting with low pulsed-laser powers. However, when the excitation power increases, the single exponential decay suffers

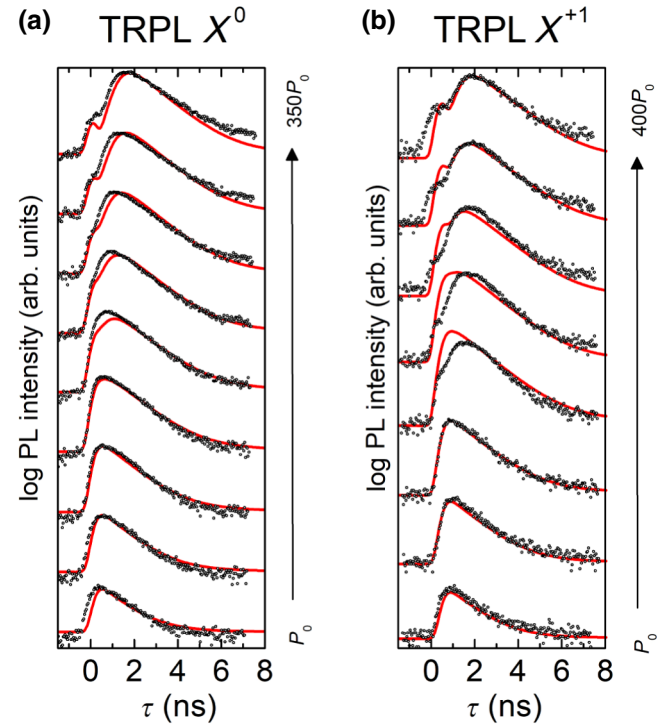
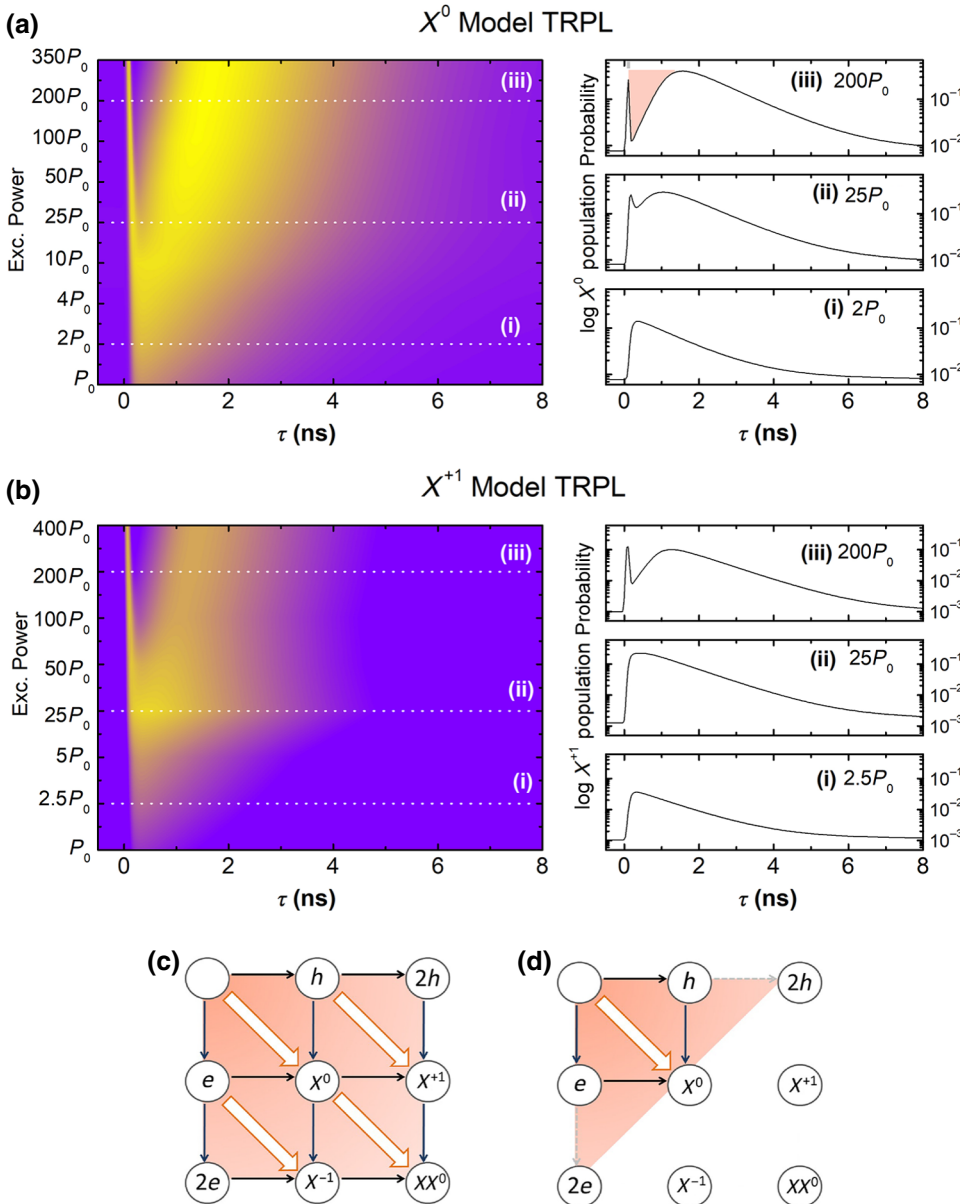


FIG. 2. Experimental measurement of TRPL (open circles) and model simulation of the time evolution of the population probability (red continuous lines) as a function of the pulsed excitation power for a neutral exciton (X^0) (a) and a positive trion (X^{+1}) (b). In each case, $P_0 = 9$ nW (a) and $P_0 = 8$ nW (b). The output of the model includes the convolution with the system time response.

a significant delay and a first and fast ($< \text{ns}$) optical emission is detected. The presence of this double-peaked decay is independent of the QD microstate. The simulation of the occupation probability for both X^0 and X^{+1} over time under pulsed excitation reproduces the experimental TRLP curves well, using the model output parameters found in the previous steady-state modeling. In order to reproduce the experimental time resolution, the model output is convoluted with a Gaussian function with a full width at half maximum (FWHM) of 400 ps. However, as expected, the agreement for X^{+1} is worse, as the saturation behavior for this state is overestimated in our model. Despite this saturation discrepancy, the model output reproduces the double-transient PL structure found in both X^0 and X^{+1} states within the power-excitation range used in the experiment.



V. DISCUSSION AND CONCLUSIONS

Figures 3(a) and 3(b) show the power dependence of the X^0 and X^{+1} population probabilities, given by the output of the model applied to the experimental results in Fig. 2, before applying the Gaussian convolution to include the effect of the experimental system response. As such, it shows the actual, underlying carrier dynamics of the QD. As can be seen, our simple model reproduces the existence of two time-differentiated dynamical stages in the QD-carrier capture and recombination, when the QD is pumped with high power. The first and fast decay follows the time dependence of the laser pulse (Gaussian profile, FWHM ~ 100 ps) and is highly influenced by the exciton capture time (τ_X) and the WL-reservoir decay time (τ_W). As τ_W increases, there are two strong effects: the delay

FIG. 3. The time evolution of the neutral-exciton-microstate probability as a function of the pulsed-excitation power as direct output from the model, not including the convolution with the system response. (a) The TRPL simulation for the X^0 population. On the right are plots corresponding to the time traces labeled as (i), (ii), and (iii) on the left-hand density plot ($P_0 = 9$ nW). (b) The TRPL simulation for the X^{+1} population. On the right are plots corresponding to the time traces labeled as (i), (ii), and (iii) on the left-hand density plot ($P_0 = 8$ nW). (c),(d) The model scheme under pulsed excitation for the neutral-exciton (X^0) population. During the first stage after the pulse excitation, the QD population increases very quickly (represented as the red shaded area under the model scheme) and the excitonic transition decay is mostly dominated by the various carrier-capture processes as shown in (c). However, as soon as the mean QD population has decreased due to the carrier-relaxation processes, the X^0 population is mostly influenced by its intrinsic radiative decay. The multiple microstate configurations and their own dynamical evolution with the excitation power are manifested as an evolving effective decay, which is observed in each of the QD excitonic transitions.

time between the first transient spike and the second peak increases and the contrast between the two peaks increases. As the exciton capture time increases, the time between the two peaks decreases slightly, while the contrast between the two peaks is reduced significantly. These results hold for the positive and negative trion populations, as well as the exciton population, although the exact dynamics depend on the other time constants, the G_a/G_b ratio, and the excitation powers. For the experimental parameters given in Table I, increasing τ_w from 50 ps to 300 ps increases the spacing between the two PL transients from 0.7 to 2.0 ns, while increasing the contrast from 0% to 50% at low powers and from 20% to 80% at high powers. As the exciton-capture time increases from 5 ps to 200 ps, the contrast between the two peaks disappears at all but the highest powers.

In previous spectrally resolved analyses, the first fast decay has been measured and linked to broad background optical emission that is present when pumping in high-excitation conditions [45,48]. This broad background emission has been explained as the result of biexciton Coulombic interaction with excitons present in a 2D reservoir [73]. The background spectrum dominates the PL emission during a first stage, while the characteristic narrow QD-excitonic recombination transitions are recovered in a later stage [35,73]. This effect is dominant for QDs with exciton and biexciton radiative lifetimes of the same order as the 2D reservoir radiative lifetime, as is the case for GaAs QDs ($\tau_d^{X^0}, \tau_d^{XX^0} \sim 100$ ps). However, for QDs with longer excitonic radiative decays, as in the InAs QDs studied in our present work ($\tau_d^{X^0} \sim 1$ ns), the expected contribution of this kind of interaction is weaker [73]. Furthermore, this model only predicts background emission red shifted to the biexciton transition, but the double-peaked structure and the broad background have been measured across the entire single QD spectrum (above and below the biexciton transition).

In our time-resolved analysis, we show that a network of QD microstates (single carriers, two carriers, neutral exciton, positive and negative trion, and neutral biexciton) connected to a 2D reservoir reproduces the two different dynamical stages: a first stage dominated by carrier capture from the WL reservoir and its radiative relaxation (providing ultrafast dynamics) and a second stage dominated by the corresponding microstate radiative decay. Although our analysis does not provide any insight into the spectral features of the first fast decay, our model reproduces this feature for different microstate configurations, thus being independent of the number of carriers. This finding is compatible with a broad background emission covering the entire QD spectrum and characterized by fast radiative decay [45,48].

The fast decay and its associated background transition should be a relevant feature when considering the single-photon purity characteristics of the excitonic emission

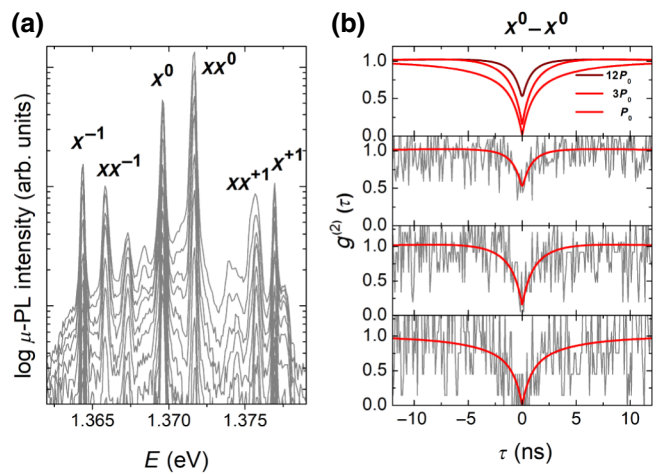


FIG. 4. (a) Microphotoluminescence spectra as a function of the 790-nm cw excitation power in a second quantum dot and its corresponding transition labeling ($P_0 = 140$ nW). (b) The photon-autocorrelation measurement of the neutral exciton (X^0) optical emission as a function of the 790-nm cw excitation power, from the same QD as in (a) ($P_0 = 280$ nW). The red continuous lines show the best model fit for each power. As the power increases, the single-photon purity, characterized by the $g^{(2)}(0)$ value, changes from 0.02 (P_0) to 0.34 ($3 \times P_0$) and 0.53 ($12 \times P_0$). The top panel shows the model output for comparison.

in a QD. If the background contribution is related to microstate-cascade recombination, any possible spectral overlap could affect the single-photon purity characteristics of the postselected optical emission. This hypothesis is bolstered by second-order correlation function measurements that we make on a second quantum dot, which show a decrease in the single-photon purity as the power is increased. Figure 4(a) shows cw power-dependent μ -PL spectra with a logarithmic scale on the integrated intensity axis. As shown, as the cw excitation power is increased, the QD spectrum acquires a broadband background over the entire spectral range. We perform $g^{(2)}(\tau)$ photon-correlation measurements as a function of the cw power, filtering the X^0 transition from the quantum dot in Fig. 4(a) and fitted with a simple model [63] to extract the $g^{(2)}(0)$ values. In the fitting, we include the convolution with a Gaussian function (FWHM = 400 ps) to account for the finite system time response. As shown in Fig. 4(b), the second-order correlation function can go to approximately zero at low power, while the antibunching is significantly reduced ($g^{(2)}(0) > 0.5$) at higher cw excitation powers.

We note that in a typical μ -PL-spectrum acquisition, one usually integrates over more than 10^{10} single QD recombinations ($\tau_d \sim 1$ ns), assuming zero photon losses and ideal detector efficiency. This means that we see the average behavior of the system when performing a single spectrum acquisition and photon-correlation histograms. The presence of the fast peak does not indicate that all decay paths from a PL measurement undergo such a decay; this would

only be the case if the model predicted zero probability of other states at the time. Higher power results in an increase in contrast of this fast decay, as the spike arises from removing population from lower-order complexes and moving it to higher-order complexes, and this becomes relatively more efficient as the excitation power increases. We tentatively assume that the double-peak TRPL structure will be more intense for QD systems with a larger number of available microstates. The reduction of the available microstates will decrease the time required to saturate the entire microstate ensemble and reduce the available carrier configurations. However, in order to elucidate the possible different microscopic physical origins of these two stages, to include specific information about the spectral characteristics of the emission, and to provide more insights into the possible negative effects on the single-photon emission features, a more sophisticated model must be developed.

Despite the possible negative consequences of the double-peaked decay in the QD optical emission, this complex dynamical evolution can be used to create fast all-optical switching of the single-photon emission from a single-semiconductor QD. The fast modulation of the optical emission from the microstate population refilling can be used as a physical mechanism to force sub-nanosecond optical depletion and consecutive fast refilling to the different QD excitonic transitions. The reddish shade in Fig. 3(a) (upper right panel) shows the time-zone influence of the fast population-depletion recovery process for the X^0 microstate. A pulsed nonresonant light excitation acting as the transistor gate can modulate the QD excitonic population and its single-photon emission when it is optically driven by an adjacent cw LED pumping.

In conclusion, our time-resolved study of single-QD optical emission allows us to determine the effect of the WL and QD interaction by two capture processes, namely correlated and uncorrelated electron and hole captures. This is equivalent to producing synchronous and nonsynchronous electron and hole capture. The specific values of the capture and decay time constants and pumping ratios determine the final injection dynamics between the WL and the QD microstate system. Our model suggests that the system has two distinct phases of time evolution—a first subnanosecond decay peak and a second longer decay, in agreement with the literature. The first peak is governed by the WL dynamics, while the second is governed by the particular microstate decay. From our analysis, we can conclude that the potentially undesirable effect of the double-peaked time transient should be more important in QDs with a higher number of available microstates, where state-refilling processes through microstates are dominant. However, this ultrafast carrier redistribution could also offer another route to the design of single-photon transistor operation for nonresonant pumped schemes—such as,

for example, the slave counterparts in proposals for hybrid optical and/or electrical devices [25].

ACKNOWLEDGMENTS

This work was partially funded by the Australian Research Council Centre of Excellence for Engineered Quantum Systems (Grant No. CE170100009).

- [1] I. A. Walmsley, Quantum optics: Science and technology in a new light, *Science* **348**, 525 (2015).
- [2] A. J. Shields, Semiconductor quantum light sources, *Nat. Photonics* **1**, 215 (2007).
- [3] S. Buckley, K. Rivoire, and J. Vučković, Engineered quantum dot single-photon sources, *Rep. Prog. Phys.* **75**, 126503 (2012).
- [4] P. Lodahl, S. Mahmoodian, and S. Stobbe, Interfacing single photons and single quantum dots with photonic nanostructures, *Rev. Mod. Phys.* **87**, 347 (2015).
- [5] N. Somaschi, V. Giesz, L. De Santis, J. C. Loredo, M. P. Almeida, G. Hornecker, S. L. Portalupi, T. Grange, C. Anton, J. Demory, C. Gomez, I. Sagnes, N. D. Lanzillotti-Kimura, A. Lemaitre, A. Aufcèves, A. G. White, L. Lanço, and P. Senellart, Near-optimal single-photon sources in the solid state, *Nat. Photonics* **10**, 340 (2016).
- [6] Y.-M. He, Y. He, Y.-J. Wei, D. Wu, M. Atatüre, C. Schneider, S. Höfling, M. Kamp, C.-Y. Lu, and J.-W. Pan, On-demand semiconductor single-photon source with near-unity indistinguishability, *Nat. Nanotechnol.* **8**, 213 (2013).
- [7] C. Kammerer, C. Voisin, G. Cassabois, C. Delalande, Ph. Roussignol, F. Klopf, J. P. Reithmaier, A. Forchel, and J. M. Gérard, Line narrowing in single semiconductor quantum dots: Toward the control of environment effects, *Phys. Rev. B* **66**, 041306(R) (2002).
- [8] Y. Ducommun, M. Kroutvar, M. Reimer, M. Bichler, D. Schuh, G. Abstreiter, and J. J. Finley, Redistribution dynamics of optically generated charges in In(Ga)As/GaAs self-assembled quantum dots, *Appl. Phys. Lett.* **85**, 2592 (2004).
- [9] C. Cornet, C. Platz, P. Caroff, J. Even, C. Labbé, H. Folliot, A. Le Corre, and S. Loualiche, Approach to wetting-layer-assisted lateral coupling of InAs/InP quantum dots, *Phys. Rev. B* **72**, 035342 (2005).
- [10] S. Sanguinetti, K. Watanabe, T. Tateno, M. Gurioli, P. Werner, M. Wakaki, and N. Koguchi, Modified droplet epitaxy GaAs/AlGaAs quantum dots grown on a variable thickness wetting layer, *J. Cryst. Growth.* **253**, 71 (2003).
- [11] M. Shahzadeh and M. Sabaeian, The effects of wetting layer on electronic and optical properties of intersubband p -to- s transitions in strained dome-shaped InAs/GaAs quantum dots, *AIP Adv.* **4**, 067113 (2014).
- [12] W. Yang, R. R. Lowe-Webb, H. Lee, and P. C. Sercel, Effect of carrier emission and retrapping on luminescence time decays in InAs/GaAs quantum dots, *Phys. Rev. B* **56**, 13314 (1997).
- [13] S. Sanguinetti, M. Henini, M. Grassi Alessi, M. Capizzi, P. Frigeri, and S. Franchi, Carrier thermal escape and

- retrapping in self-assembled quantum dots, *Phys. Rev. B* **60**, 8276 (1999).
- [14] C. Lobo, R. Leon, S. Marcinkevičius, W. Yang, P. C. Sercel, X. Z. Liao, J. Zou, and D. J. H. Cockayne, Inhibited carrier transfer in ensembles of isolated quantum dots, *Phys. Rev. B* **60**, 16647 (1999).
- [15] G. Muñoz-Matutano, I. Suárez, J. Canet-Ferrer, B. Alén, D. Rivas, L. Seravalli, G. Trevisi, P. Frigeri, and J. Martínez-Pastor, Size dependent carrier thermal escape and transfer in bimodally distributed self assembled InAs/GaAs quantum dots, *J. Appl. Phys.* **111**, 123522 (2012).
- [16] S. Hinooda, S. Loualiche, B. Lambert, N. Bertru, M. Paillard, X. Marie, and T. Amand, Wetting layer carrier dynamics in InAs/InP quantum dots, *Appl. Phys. Lett.* **78**, 3052 (2001).
- [17] M. Ohmori, P. Vitushinskiy, and H. Sakaki, Diffusion process of excitons in the wetting layer and their trapping by quantum dots in sparsely spaced InAs quantum dot systems, *Appl. Phys. Lett.* **98**, 133109 (2011).
- [18] D. R. Matthews, H. D. Summers, P. M. Smowton, and M. Hopkinson, Experimental investigation of the effect of wetting-layer states on the gain-current characteristic of quantum-dot lasers, *Appl. Phys. Lett.* **81**, 4904 (2002).
- [19] D. R. Matthews, H. D. Summers, P. M. Smowton, P. Blood, P. Rees, and M. Hopkinson, Dynamics of the wetting-layer-quantum-dot interaction in InGaAs self-assembled systems, *IEEE J. Quantum Electron.* **41**, 344 (2005).
- [20] C. Wang, F. Grillot, and J. Even, Impacts of wetting layer and excited state on the modulation response of quantum-dot lasers, *IEEE J. Quantum Electron.* **48**, 1144 (2012).
- [21] Y. B. Ezra, B. I. Lembrikov, and M. Haridim, Ultrafast all-optical processor based on quantum-dot semiconductor optical amplifiers, *IEEE J. Quantum Electron.* **45**, 34 (2009).
- [22] E. Stock, F. Albert, C. Hopfmann, M. Lermer, C. Schneider, S. Höfling, A. Forchel, M. Kamp, and S. Reitzenstein, On-chip quantum optics with quantum dot microcavities, *Adv. Mater.* **25**, 707 (2012).
- [23] J. P. Lee, E. Murray, A. J. Bennett, D. J. P. Ellis, C. Dangel, I. Farrer, P. Spencer, D. A. Ritchie, and A. J. Shields, Electrically driven and electrically tunable quantum light sources, *Appl. Phys. Lett.* **110**, 071102 (2017).
- [24] P. Munnely, T. Heindel, A. Thoma, M. Kamp, S. Höfling, C. Schneider, and S. Reitzenstein, Electrically tunable single-photon source triggered by a monolithically integrated quantum dot microlaser, *ACS Photonics* **4**, 790 (2017).
- [25] B. Alén, D. Fuster, Y. González, and L. González, in *Proceedings SPIE, Quantum Photonic Devices 2018* (SPIE Nanoscience + Engineering, San Diego, California, United States, 2018), Vol. 10733.
- [26] R. Enzmann, C. Jendrysiak, C. Seidl, A. Heindl, D. Baierl, G. Bohm, R. Meyer, J. Finley, and M. Amann, in *2008 8th IEEE Conference on Nanotechnology* (IEEE Service Center, Piscataway, NJ, 2008), p. 67.
- [27] H. Stolz, ed., *Time-Resolved Light Scattering from Excitons* (Springer-Verlag, Berlin, Heidelberg, 1994).
- [28] A. J. Ramsay, A review of the coherent optical control of the exciton and spin states of semiconductor quantum dots, *Semicond. Sci. Technol.* **25**, 103001 (2010).
- [29] C. Santori, G. S. Solomon, M. Pelton, and Y. Yamamoto, Time-resolved spectroscopy of multiexcitonic decay in an InAs quantum dot, *Phys. Rev. B* **65**, 073310 (2002).
- [30] B. Patton, W. Langbein, and U. Woggon, Trion, biexciton, and exciton dynamics in single self-assembled cdse quantum dots, *Phys. Rev. B* **68**, 125316 (2003).
- [31] E. Dekel, D. V. Regelman, D. Gershoni, E. Ehrenfreund, W. V. Schoenfeld, and P. M. Petroff, Cascade evolution and radiative recombination of quantum dot multiexcitons studied by time-resolved spectroscopy, *Phys. Rev. B* **62**, 11038 (2000).
- [32] T. Kuroda, S. Sanguinetti, M. Gurioli, K. Watanabe, F. Minami, and N. Koguchi, Picosecond nonlinear relaxation of photojected carriers in a single GaAs/Al_{0.3}Ga_{0.7}As quantum dot, *Phys. Rev. B* **66**, 121302(R) (2002).
- [33] P. A. Dalgarno, J. M. Smith, J. McFarlane, B. D. Gerardot, K. Karrai, A. Badolato, P. M. Petroff, and R. J. Warburton, Coulomb interactions in single charged self-assembled quantum dots: Radiative lifetime and recombination energy, *Phys. Rev. B* **77**, 245311 (2008).
- [34] P. Borri, V. Cesari, and W. Langbein, Measurement of the ultrafast gain recovery in InGaAs/GaAs quantum dots: Beyond a mean-field description, *Phys. Rev. B* **82**, 115326 (2010).
- [35] Ü. Bockelmann, W. Heller, A. Filoromo, and Ph. Roussignol, Microphotoluminescence studies of single quantum dots. I. Time-resolved experiments, *Phys. Rev. B* **55**, 4456 (1997).
- [36] J. Szczytko, L. Kappei, J. Berney, F. Morier-Genoud, M. T. Portella-Oberli, and B. Deveaud, Determination of the Exciton Formation in Quantum Wells from Time-Resolved Interband Luminescence, *Phys. Rev. Lett.* **93**, 137401 (2004).
- [37] V. Cesari, W. Langbein, and P. Borri, Dephasing of excitons and multiexcitons in undoped and *p*-doped InAs/GaAs quantum dots-in-a-well, *Phys. Rev. B* **82**, 195314 (2010).
- [38] P. Borri, S. Schneider, W. Langbein, and D. Bimberg, Ultrafast carrier dynamics in InGaAs quantum dot materials and devices, *J. Optics A: Pure Appl. Optics* **8**, S33 (2006).
- [39] P. Borri, W. Langbein, S. Schneider, U. Woggon, R. L. Sellin, D. Ouyang, and D. Bimberg, Ultralong Dephas-ing Time in InGaAs Quantum Dots, *Phys. Rev. Lett.* **87**, 157401 (2001).
- [40] M. Gurioli, A. Vinattieri, M. Zamfirescu, M. Colocci, S. Sanguinetti, and Richard Nötzel, Recombination kinetics of InAs quantum dots: Role of thermalization in dark states, *Phys. Rev. B* **73**, 085302 (2006).
- [41] B. Alloing, C. Zinoni, L. H. Li, and A. Fiore, Structural and optical properties of low-density and In-rich InAs GaAs quantum dots, *J. Appl. Phys.* **101**, 024918 (2007).
- [42] T. E. J. Campbell-Ricketts, N. A. J. M. Kleemans, R. Nötzel, A. Yu. Silov, and P. M. Koenraad, The role of dot height in determining exciton lifetimes in shallow InAs/GaAs quantum dots, *Appl. Phys. Lett.* **96**, 033102 (2010).
- [43] J. Johansen, S. Stobbe, I. S. Nikolaev, T. Lund-Hansen, P. T. Kristensen, J. M. Hvam, W. L. Vos, and P. Lodahl, Size dependence of the wavefunction of self-assembled InAs quantum dots from time-resolved optical measurements, *Phys. Rev. B* **77**, 073303 (2008).

- [44] L. Dusanowski, M. Gawełczyk, J. Misiewicz, S. Höfling, J. P. Reithmaier, and G. Sek, Strongly temperature-dependent recombination kinetics of a negatively charged exciton in asymmetric quantum dots at $1.55\text{ }\mu\text{m}$, *Appl. Phys. Lett.* **23**, 043103 (2018).
- [45] B. Zinoni, C. Alloing, C. Monat, L. H. Li, L. Lunghi, A. Gerardino, and A. Fiore, Time resolved measurements on low-density single quantum dots at 1300 nm , *Phys. Stat. Sol. c* **3**, 3717 (2006).
- [46] G. Muñoz-Matutano, D. Rivas, A. L. Ricchiuti, D. Barrera, C. R. Fernández-Pousa, J. Martínez-Pastor, L. Seravalli, G. Trevisi, P. Frigeri, and S. Sales, Time resolved emission at 1.3 m of a single InAs quantum dot by using a tunable fibre Bragg grating, *Nanotechnology* **25**, 035204 (2014).
- [47] E. Dekel, D. V. Regelman, D. Gershoni, E. Ehrenfreund, W. V. Schoenfeld, and P. M. Petroff, Radiative lifetimes of single excitons in semiconductor quantum dots—manifestation of the spatial coherence effect, *Solid State Communications* **117**, 395 (2001).
- [48] N. Chauvin, C. Zinoni, M. Francardi, A. Gerardino, L. Balet, B. Alloing, L. H. Li, and A. Fiore, Controlling the charge environment of single quantum dots in a photonic-crystal cavity, *Phys. Rev. B* **80**, 241306(R) (2009).
- [49] D. Elvira, R. Hostein, B. Fain, L. Monniello, A. Michon, G. Beaudoin, R. Braive, I. Robert-Philip, I. Abram, I. Sagnes, and A. Beveratos, Single $\text{InAs}_{1-x}p_x/\text{InP}$ quantum dots as telecommunications-band photon sources, *Phys. Rev. B* **84**, 195302 (2011).
- [50] K. C. Hall, E. J. Koerperick, T. F. Boggess, O. B. Shchekin, and D. G. Deppe, Hole spin relaxation in neutral InGaAs quantum dots: Decay to dark states, *Appl. Phys. Lett.* **90**, 053109 (2007).
- [51] C. Becher, A. Kiraz, P. Michler, A. Imamoglu, W. V. Schoenfeld, P. M. Petroff, Lidong Zhang, and E. Hu, Nonclassical radiation from a single self-assembled InAs quantum dot, *Phys. Rev. B* **63**, 121312(R) (2001).
- [52] D. V. Regelman, U. Mizrahi, D. Gershoni, E. Ehrenfreund, W. V. Schoenfeld, and P. M. Petroff, Semiconductor Quantum Dot: A Quantum Light Source of Multicolor Photons with Tunable Statistics, *Phys. Rev. Lett.* **87**, 257401 (2001).
- [53] L. Seravalli, C. Bocchi, G. Trevisi, and P. Frigeri, Properties of wetting layer states in low density InAs quantum dot nanostructures emitting at 1.3 m : Effects of InGaAs capping, *J. Appl. Phys.* **108**, 114313 (2010).
- [54] G. Trevisi, L. Seravalli, P. Frigeri, and S. Franchi, Low density $\text{InAs}/(\text{In})\text{GaAs}$ quantum dots emitting at long wavelengths, *Nanotechnology* **20**, 415607 (2009).
- [55] P. Frigeri, L. Nasi, M. Prezioso, L. Seravalli, G. Trevisi, E. Gombia, R. Mosca, F. Germini, C. Bocchi, and S. Franchi, Effects of the quantum dot ripening in high-coverage InAs/GaAs nanostructures, *J. Appl. Phys.* **102**, 083506 (2007).
- [56] G. Muñoz-Matutano, B. Alén, J. Martínez-Pastor, L. Seravalli, P. Frigeri, and S. Franchi, Selective optical pumping of charged excitons in unintentionally doped InAs quantum dots, *Nanotechnology* **19**, 145711 (2008).
- [57] E. S. Moskalenko, V. Donchev, K. F. Karlsson, P. O. Holtz, B. Monemar, W. V. Schoenfeld, J. M. Garcia, and P. M. Petroff, Effect of an additional infrared excitation on the luminescence efficiency of a single InAs/GaAs quantum dot, *Phys. Rev. B* **68**, 155317 (2003).
- [58] M. Kaniewska and O. Engström, Deep traps at GaAs/GaAs interface grown by MBE-interruption growth technique, *Mater. Sci. Eng.: C* **27**, 1069 (2007).
- [59] J. F. Chen, C. H. Yang, R. M. Hsu, and U. S. Wang, Influence of thermal annealing on the electron emission of InAs quantum dots containing a misfit defect state, *J. Appl. Phys.* **105**, 063705 (2009).
- [60] S. Golovynskyi, O. Datsenko, L. Seravalli, O. Kozak, G. Trevisi, P. Frigeri, I. S. Babichuk, I. Golovynska, and J. Qu, Deep levels in metamorphic InAs/InGaAs quantum dot structures with different composition of the embedding layers, *Semicond. Sci. Technol.* **32**, 125001 (2017).
- [61] J. C. Rimada, M. Prezioso, L. Nasi, E. Gombia, R. Mosca, G. Trevisi, L. Seravalli, P. Frigeri, C. Bocchi, and S. Franchi, Electrical and structural characterization of InAs/InGaAs quantum dot structures on GaAs, *Mater. Sci. Eng.: B* **165**, 111 (2009).
- [62] J. Gomis-Bresco, G. Muñoz-Matutano, J. Martínez-Pastor, B. Alén, L. Seravalli, P. Frigeri, G. Trevisi, and S. Franchi, Random population model to explain the recombination dynamics in single InAs/GaAs quantum dots under selective optical pumping, *New J. Phys.* **13**, 023022 (2011).
- [63] D. Rivas, G. Muñoz-Matutano, J. Canet-Ferrer, R. García-Calzada, G. Trevisi, L. Seravalli, P. Frigeri, and J. Martínez-Pastor, Two-color single-photon emission from InAs quantum dots: Toward logic information management using quantum light, *Nano Lett.* **14**, 456 (2014).
- [64] A. Hartmann, Y. Ducommun, E. Kapon, U. Hohenester, and E. Molinari, Few-Particle Effects in Semiconductor Quantum Dots: Observation of Multicharged Excitons, *Phys. Rev. Lett.* **84**, 5648 (2000).
- [65] M. H. Baier, A. Malko, E. Pelucchi, D. Y. Oberli, and E. Kapon, Quantum-dot exciton dynamics probed by photon-correlation spectroscopy, *Phys. Rev. B* **73**, 205321 (2006).
- [66] G. R. Dennis, J. J. Hope, and M. T. Johnsson, Xmds2: Fast, scalable simulation of coupled stochastic partial differential equations, *Comput. Phys. Commun.* **94**, 201 (2013).
- [67] T. Kazimierczuk, M. Goryca, M. Koperski, A. Golnik, J. A. Gaj, M. Nawrocki, P. Wojnar, and P. Kossacki, Picosecond charge variation of quantum dots under pulsed excitation, *Phys. Rev. B* **81**, 155313 (2010).
- [68] H. Nakajima, H. Kumano, H. Iijima, S. Odashima, and I. Suemune, Carrier-transfer dynamics between neutral and charged excitonic states in a single quantum dot probed with second-orderphoton correlation measurements, *Phys. Rev. B* **88**, 045324 (2013).
- [69] M. Grundmann and D. Bimberg, Theory of random population for quantum dots, *Phys. Rev. B* **55**, 9740 (1997).
- [70] M. Ediger, G. Bester, A. Badolato, P. M. Petroff, K. Karrai, A. Zunger, and R. J. Warburton, Peculiar many-body effects revealed in the spectroscopy of highly charged quantum dots, *Nat. Phys.* **3**, 774 (2007).
- [71] K. F. Karlsson, D. Y. Oberli, M. A. Dupertuis, V. Troncale, M. Byszewski, E. Pelucchi, A. Rudra, P. O. Holtz, and E. Kapon, Spectral signatures of high-symmetry quantum dots and effects of symmetry breaking, *New J. Phys.* **17**, 103017 (2015).

- [72] M. R. Molas, A. A. L. Nicolet, B. Piętka, A. Babinski, and M. Potemski, The excited spin-triplet state of a charged exciton in quantum dots, *J. Phys.: Condens. Matter* **28**, 365301 (2016).
- [73] P. Senellart, E. Peter, J. Hours, A. Cavanna, and J. Bloch, Few particle effects in the emission of short-radiative-lifetime single quantum dots, *Phys. Rev. B* **72**, 115302 (2005).